LAWRENCE
LIVERMORE
NATIONAL
LABORATORY

UCRL-JRNL-234943

Soft Phonons in (delta)-Phase Plutonium Near the (delta)-(alpha)' Transition

R. Xu, J. Wong, P. Zshack, H. Hong, T.-C. Chiang

September 25, 2007

Europhysics Letters (EPL)

Updated October 14, 2003

Soft Phonons in δ-Phase Plutonium near the δ-α' Transition

Ruqing Xu,[1,2] Joe Wong,[3*] Paul Zschack,[4] Hawoong Hong,[2] and T.-C. Chiang[1,2]

[1]Department of Physics, University of Illinois at Urbana-Champaign, 1110 W. Green Street, Urbana, Illinois 61801

[2]Frederick Seitz Materials Research Laboratory, University of Illinois at Urbana-Champaign, 104 S. Goodwin Avenue, Urbana, Illinois 61801

[3]Lawrence Livermore National Laboratory, University of California, P.O. Box 808, Livermore, California 94551

[4]Advanced Photon Source, Argonne National Laboratory, Argonne, Illinois 60439

Plutonium and its alloys exhibit complex phase diagrams that imply anomalous lattice dynamics near phase stability boundaries. Specifically, the TA [111] phonon branch in Ga-stabilized δ-Pu at room temperature shows a pronounced soft mode at the zone boundary, which suggests a possible connection to the martensitic transformation from the fcc δ-phase to the monoclinic α'-phase at low temperatures. This work is a study of the lattice dynamics of this system by x-ray thermal diffuse scattering. The results reveal little temperature dependence of the phonon frequencies, thus indicating that kinetic phonon softening is not responsible for this phase transition.

PACS: 61.10.Eq, 63.20.Dj, 64.70.Kb, 78.70.Ck

Plutonium is the most complex metallic element [1,2]. As its 5f electrons are on the verge of being either localized or itinerant, it undergoes a number of phase transitions under moderate temperature and pressure variations. Its lack of thermal and mechanical stability is a key engineering concern and poses fundamental questions about the interatomic bonding forces. Most applications of Pu employ alloying to shift the phase boundaries in order to stabilize the malleable fcc δ–phase near room temperature. In the present study, we focus on a Pu alloy containing 0.6 wt% Ga. This material is in the δ–phase at room temperature, but transforms into a monoclinic α' phase at ~170 K [1,2,3,4,5]. The present work is an investigation of the lattice dynamics of this material as its temperature is lowered toward the δ–α' transition. The technique employed is x-ray thermal diffuse scattering (TDS) which is sensitive to changes in phonon dispersion relations [6,7,8,9,10]. As the phonon dispersion relations are directly related to interatomic forces, the measurements provide a basis for understanding the phase instability in terms of changes in atomic bonding.

Prior inelastic x-ray scattering measurements carried out at room temperature on the same material revealed a pronounced soft phonon mode in the TA [111] branch at the Brillouin zone boundary (L point), which was suggested to be key to the δ–α' transition [11,12]. The same soft mode was seen in theoretical calculations and other experiments [13,14]. The α'-phase is essentially a distorted hcp structure, which can be obtained from the fcc δ-phase through a reshuffling of the (111) close-packed atomic planes from an ABC stacking sequence to an ABAB sequence. Such a transition path is consistent with the observed lattice relationships: $(111)_{\delta} \parallel (020)_{\alpha'}$ and $[-110]_{\delta} \parallel [100]_{\alpha'}$ [4] A force constant analysis shows that a soft TA mode at the L point implies a weak restoring force for sliding

motions of (111) atomic planes in the δ-phase, which would be conducive to the formation of the α'-phase. Thus, a reasonable conjecture is that the soft mode at the L point would soften further as the temperature is lowered until the restoring force is too low to resist the layer sliding transformation into the α'-phase [11,12]. While highly plausible, this conjecture has never been tested mainly due to experimental difficulties. Our results, to be presented below, show that this conjecture does not stand the test. Thus, the nature of the δ–α' phase transition must be reconsidered from an entirely different perspective.

In our experiments, a Pu sample containing 0.6 wt% Ga was prepared at the Lawrence Livermore National Laboratory. The alloy was compressed uniaxially and annealed in vacuum to promote crystallite growth [15]. The resulting polycrystalline sample was machined down to 2.8 mm in diameter and ~12 μm in thickness, and it was immediately coated with polyimide for protection from oxidation. The sample was sealed in an aluminum chamber for safety reasons. The assembly was mounted on the cold finger of a closed-cycle helium cryostat. The sample temperature was controlled by a built-in heater, a silicon diode temperature sensor, and a feedback system. The x-ray measurements were performed at the undulator beamline of sector 33, Advanced Photon Source, Argonne National Laboratory. The beam energy, set at 18.0 keV, was just below the Pu L_3 edge at 18.056 keV, but it was sufficiently high for substantial x-ray transmission though the Pu sample and the aluminum chamber walls. A pair of Kirkpatrick-Baez mirrors was employed to focus the beam to the size of 8 μm × 8 μm.

Systematic scans over the sample were performed to map the domain structure. Two especially large crystallites oriented in the (111) and (110) directions, respectively, were

found, each with an average diameter of about 50 μm. During the TDS measurements from these crystallites, the sample position was readjusted for each temperature setting to compensate for changes in physical dimensions of the system caused by thermal expansion or contraction. Transmission TDS images were recorded with an image plate detector. The lowest sample temperature during the experiment was 200 K. A 30 K safety margin from the δ–α' transition at ~170 K was maintained to avoid irreversible domain structure changes at the transition. Total exposure times of TDS images were in the range of 50 to 200 min at each temperature. The long integration times led to excellent data statistics.

Figures 1(a) and 1(b) are TDS images obtained at 307 K for the (111) and (110) grains, respectively, and Figs. 1(c) and 1(d) are the same at 200 K. All images were presented using a logarithmic intensity scale in order to show the rich structures over many decades of intensity levels. The dark circle at the center of each image is the shadow of a beam stop. Some Debye rings are evident in the images. These arise from impurity phases in the sample and chamber components. As Pu is highly reactive and difficult to handle, we have not been able to obtain ultra-pure crystalline materials. A software algorithm was employed to mask out the Debye rings to facilitate data analysis.

Each pixel in these images corresponds to a unique momentum transfer **q** in reciprocal space. The scattering intensity, to first order, is given by

$$\frac{d}{d\Omega} I(\mathbf{q}) \propto f^2 \sum_{j=1}^{3} e^{-2M} \frac{1}{\omega_{\mathbf{q},j}} \coth\left(\frac{\hbar\omega_{\mathbf{q},j}}{k_B T}\right) \left|\mathbf{q}\cdot\mathbf{e}_{\mathbf{q},j}\right|^2 ,$$

where f is the atomic form factor, $2M$ is the Debye-Waller factor, and $\omega_{\mathbf{q},j}$ and $\mathbf{e}_{\mathbf{q},j}$ are the frequency and polarization vector of the j-th phonon mode, respectively. The hyperbolic cotangent term is the phonon population including the zero-point mode occupancy. Bright

areas in the images correspond to regions in reciprocal space with low-lying phonon modes, i.e., where the phonon populations are high. Mode softening as a function of temperature is easily detectable in the images as an increasingly brighter area around the soft mode, but no such behavior was evident from a visual inspection of the data.

Our analysis employed a fourth-neighbor Born-von Kármán force constant model to generate theoretical TDS images in both the (111) and (110) orientations for a fit to the data [6,7]. The planar force constants responsible for (111) atomic layer sliding were treated as fitting parameters, while the other force constants were held fixed at the values known from prior work [11,12]. The fitting results were therefore exclusively sensitive to the TA [111] branch. The results are shown in Figs. 1(e)-1(h) for the four cases mentioned above. The agreement is excellent except for the areas covered by the Debye rings and the beam stop, where the data were excluded from the fitting.

Figure 2(a) shows the dispersion curves for the TA [111] branch from the fits at various temperatures between 307 K and 200 K. Also included are data (circles) from prior inelastic x-ray scattering results obtained at room temperature [11,12]. Evidently, there is little or no temperature dependence. The dispersion relation shows a pronounced depression at the *L* point, corresponding to a weak restoring force against sliding motions of (111) atomic layers. Plotted in Fig. 2(b) is the frequency of this soft mode at the *L* point as a function of temperature. The lack of temperature dependence indicates that the restoring force against (111) atomic layer sliding does not weaken toward the transition temperature.

The question is then: what drives the phase transition? Within the Landau theory, the free energy of the system is a smooth function and can be expressed as an expansion in terms of the generalized coordinate ξ associated with the soft TA mode:

$$F = \alpha\xi^2 - \beta\xi^4 + \gamma\xi^6 + \ldots,$$

where α, β, and γ are positive for the present case of a first-order phase transition [16,17,18]. The standard Landau theory assumes that the first coefficient α decreases as the temperature T lowers through the transition temperature T_C. The general behavior of the free energy is illustrated in Fig. 3(a). A second minimum in F, initially above the absolute minimum at $\xi = 0$, lowers and reaches zero at T_C, and becomes the absolute minimum for $T < T_C$. An abrupt change in ξ occurs at $T = T_C$. The phonon frequency for $T > T_C$ is related to the curvature of the potential well at $\xi = 0$, or the coefficient α. A decreasing α leads to a decreasing phonon frequency and a correspondingly decreasing force constant against (111) atomic layer sliding. The evolution of the second minimum in the free energy and the softening of the phonon mode are coupled and are both driven by the temperature dependence of the coefficient α.

This standard picture describes well the physics of other systems. Specifically, there are two other fcc elemental metals, γ-cerium and β-lanthanum, that show similar soft TA [111] modes at the L point, and both undergo similar first-order transitions that can be described by (111) atomic layer sliding motions leading to a double hexagonal-close-packed structure below the transition temperature [19,20]. In both cases, significant phonon softening was observed as T approaches T_C from above, and the behavior is in good accord with that illustrated in Fig. 3(a).

For δ-phase Pu, no phonon softening as a function of temperature is observed, suggesting a different type of behavior for the free energy. For simplicity, we refer to the standard case depicted in Fig. 3(a) as type A, and the behavior of δ-phase Pu as type B. The free energy curve for the latter is illustrated in Fig. 3(b). In this case, the temperature dependence of the first coefficient α must be negligible. Instead, we assume that the second coefficient, β, increases as the temperature lowers. An increasing β lowers the free energy at large ξ, causing the second minimum to move downward, but it does not affect the harmonic frequency of the potential well at $\xi = 0$. The overall shapes of the free energy curves in Figs. 3(a) and 3(b) appear very similar. However, as highlighted by the circled areas of the curves for the two types, the potential well at $\xi = 0$ is a rigid one for type B, and a soft one for type A.

Figure 4 shows schematically the behavior of the phonon frequency as a function of temperature, assuming a linear temperature dependence of the relevant free energy coefficients. Figure 4(c) is for a prototypical second-order phase transition, in which the soft mode frequency diminishes continuously to zero as T approaches T_C according to the relation: $\omega \propto \sqrt{T - T_C}$ [16,17,18,21]. Figure 4(a) is for a first-order transition of type A, in which the phonon frequency diminishes similarly, but the transition occurs before the phonon frequency reaches zero. Figure 4(b) is for a first-order transition of type B, in which the phonon frequency remains constant above the transition temperature.

The unusual behavior of δ-Pu is likely related to the large number of 5f electronic levels near the Fermi level [1,13,22,23]. A changing temperature causes the thermal populations of the 5f levels to vary, which in turn causes the electronic structure to undergo an abrupt,

collective transformation mediated by strong electron-electron correlation. The process is somewhat akin to a partial metal-insulator transition. Such interactions can be highly nonlinear, which is consistent with the large temperature dependence of a high-order term in the free energy, as inferred from the experiment.

Our discussion above of the system free energy is limited to $T > T_C$. For $T < T_C$, there can be considerable hysteresis because of kinetic effects. In fact, a substantial fraction of the sample could be trapped in a metastable phase [5,24]. Presumably, given long enough time, the material might eventually settle down to the lowest free energy state. A free electron analysis by itself, as discussed above, is not sufficient to address this issue.

In summary, the TA [111] soft mode in δ-Pu appears to be a fairly unique case that does not fit the description based on the standard model of first-order transitions. As deduced from x-ray TDS measurements, its frequency does not soften as the temperature is lowered toward T_C. A nonlinear interaction involving a high-order term in the Landau free energy is inferred. This interaction is likely related to the rather complex behavior of the 5f electrons in this system that is yet not fully understood theoretically.

The work of TCC was supported by the US Department of Energy under grant DE-FG02-07ER46383. The work of JW was performed under the auspices of the US Department of Energy by the University of California, Lawrence Livermore National Laboratory (LLNL) under contract W-7405-Eng-48. The project 03-ERD-017 was funded by the Laboratory Directed Research and Development Program at LLNL. We acknowledge the Petroleum Research Fund, administered by the American Chemical Society, and the U.S. National Science Foundation (grant DMR-05-03323) for partial support of personnel and the

beamline operations. The Advanced Photon Source at Argonne National Laboratory is supported by the US Department of Energy, Office of Basic Energy Sciences, under contract W-31-109-ENG-38.

References

* Retired; current address: 871 El Cerro Blvd, Danville CA, 94526.

[1] *Challenges in Plutonium Science*, Los Alamos Science, Number 26, V. 1 & 2 (2000), edited by N. G. Cooper.

[2] S. S. Hecker, D. R. Harbur, and T. G. Zocco, Prog. Mater. Sci. **49**, 429 (2004).

[3] P. H. Alder, G. B. Olson, and D. S. Margolies, Acta Metall. **34**, 2053 (1986).

[4] T. G. Zocco, M. F. Stevens, P. H. Alder, R. T. Sheldon, and G. B. Olson, Acta Metall. Mater. **38**, 2275 (1990).

[5] K. J. M. Blobaum, C. R. Krenn, J. J. Haslam, M. A. Wall, A. J. Schwartz, J. N. Mitchell, and T. B. Massalski, Met. Mater. Trans. A **37**, 567 (2006).

[6] R. Xu and T.-C. Chiang, Z. Kristallogr. **220**, 1009 (2005).

[7] M. Holt, Z. Wu, H. Hong, P. Zschack, P. Jemian, J. Tischler, H. Chen, and T.-C. Chiang, Phys. Rev. Lett. **83**, 3317 (1999).

[8] M. Holt, P. Zschack, H. Hong, M. Y. Chou, and T.-C. Chiang, Phys. Rev. Lett. **86**, 3799 (2001).

[9] M. Holt, M. Sutton, P. Zschack, H. Hong, and T.-C. Chiang, Phys. Rev. Lett. **98**, 065501 (2007).

[10] J. Wong, M. Wall, A. J. Schwartz, R. Xu, M. Holt, H. Hong, P. Zschack, and T.-C. Chiang, Appl. Phys. Lett. **84**, 3747 (2004).

[11] J. Wong, M. Krisch, D. L. Farber, F. Occelli, A. J. Schwartz, T.-C. Chiang, M. Wall, C. Boro, and R. Xu, Science **301**, 1078 (2003); G. Lander, Science, **301**, 1057 (2003).

[12] J. Wong, M. Krisch, D. L. Farber, F. Occelli, R. Xu, T.-C. Chiang, D. Clatterbuck, A. J. Schwartz, M. Wall, and C. Boro, Phys. Rev. B **72**, 064115 (2005).

[13] X. Dai, S.Y. Savrasov, G. Kotliar, A. Migliori, H. Ledbetter, and E. Abrahams, Science **300**, 953 (2003).

[14] R. J. McQueeney, A. C. Lawson, A. Migliori, T. M. Kelley, B. Fultz, M. Ramos, B. Martinez, J. C. Lashley, and S. C. Vogel, Phys. Rev. Lett. **92**, 146401 (2004).

[15] J. C. Lashley, M. G. Stout, R. A. Pereyra, M. S. Blau, and J. D. Embury, Scr. Mater. **44**, 2815 (2001).

[16] W. Cochran, Phys. Rev. Lett. **3**, 412 (1959); W. Cochran, Adv. Phys. **9**, 387 (1960).

[17] P. W. Anderson, in *Fizika Dielectrikov*, edited by G. I. Skanavi (Acad. Nauk SSR, Moscow, 1960).

[18] P. Tolédano and V. Dmitriev, *Reconstructive Phase Transitions in Crystals and Quasicrystals* (World Scientific, Singapore, 1996).

[19] C. Stassis, C.-K. Loong, and O. D. McMasters, Phys. Rev. B **25**, 6485 (1982).

[20] C. Stassis, C.-K. Loong, and J. Zarestky, Phys. Rev. B **26**, 5426 (1982).

[21] For a second-order transition, the coefficient γ is typically ignored, β is assumed to be negative, and α is taken to depend linearly on temperature.

[22] S. Y. Savrasov, G. Kotliar, and E. Abrahams, Nature **410**, 793 (2001).

[23] J. H. Shim, K. Haule, and G. Kotliar, Nature **446**, 513 (2007).

[24] J. C. Lashley, J. Singleton, A. Miglior, J. B. Betts, R. A. Sisher, J. L. Smith, and R. J.

McQueeney, Phys. Rev. Lett. **91**, 205901 (2003).

Fig. 1. X-ray TDS images for (a) a (111) grain at 307K, (b) a (110) grain at 307 K, (c) a (111) grain at 200 K, and (d) a (110) grain at 200 K. The corresponding fits are shown in (e)-(h).

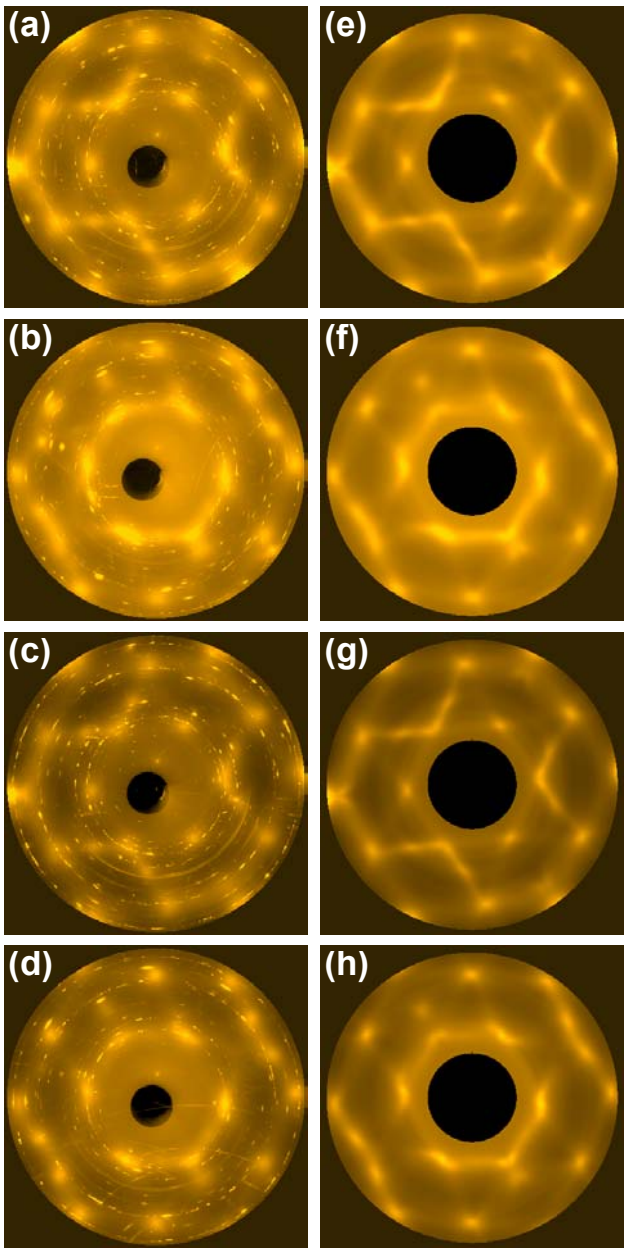

Fig. 2. (a) Phonon dispersion curves of the TA [111] branch deduced from fitting the TDS images obtained at various temperatures. The circles are data points from prior inelastic x-ray scattering (IXS) measurements. (b) The experimental phonon frequency at the *L* point as a function of temperature.

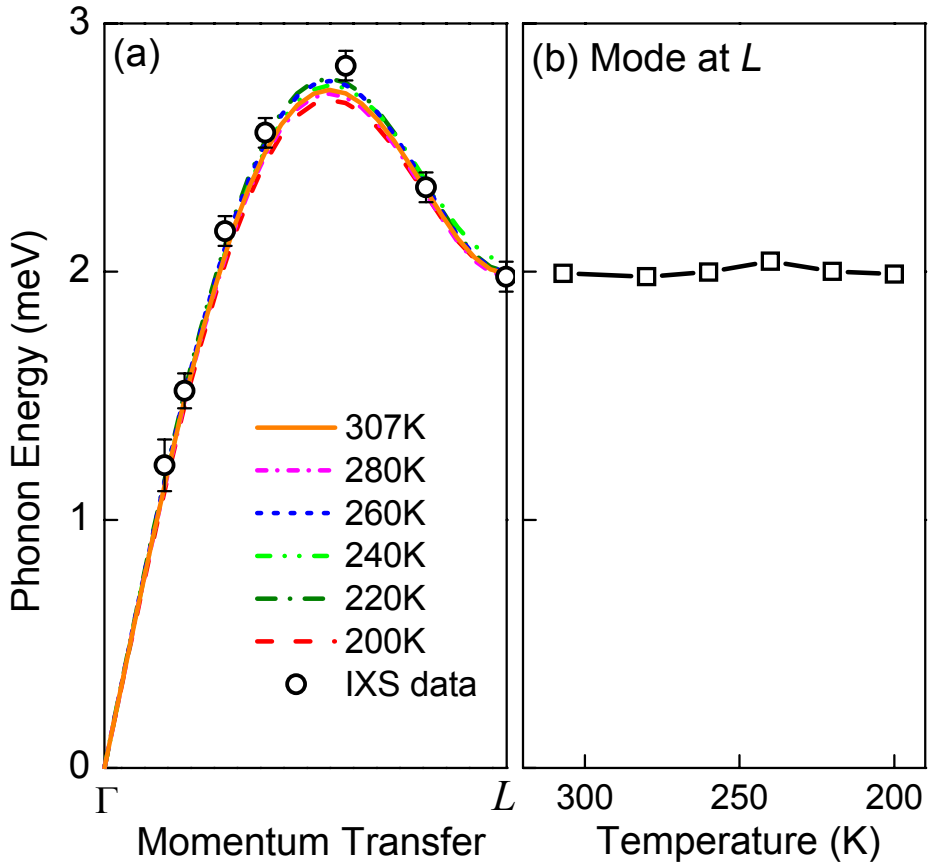

Fig. 3. Schematic diagrams of the Landau free energy curves at temperatures above, at, and below the transition temperature T_C for (a) type-A and (b) type-B first-order phase transitions.

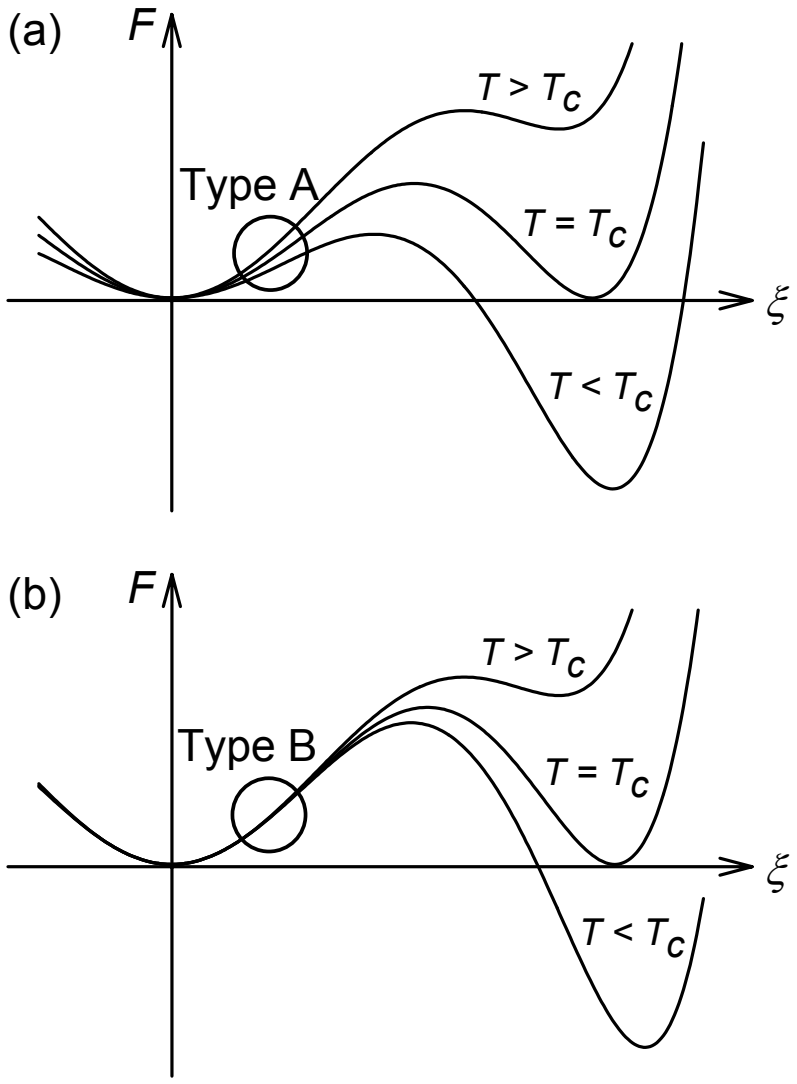

Fig. 4. Schematic diagrams showing phonon frequencies as a function of temperature for prototypical (a) type-A first-order, (b) type-B first-order, and (c) second-order phase transitions. T_0 is the temperature at which α vanishes.